CrystEngComm

Accepted Manuscript

ROYAL SOCIETY OF CHEMISTRY

www.rsc.org/crystengcomm

Cite this: DOI: 10.1039/c0xx00000x

www.rsc.org/xxxxxx

ARTICLE TYPE

Delicate modulated assembly of a new kind of trinuclear copper(II) motifs governed by N-contained agents

Shu-Ting Wu,*[a,b] Hong-Liang Tang,[a] Shu-Mei Lu,[a] Qiao-Yan Ye,[a] Xi-He Huang,[a,b] Chang-Cang Huang,[a] Xiao-Lin Hu,[a] Shou-Tian Zheng[a]

Received (in XXX, XXX) Xth XXXXXXXXX 20XX, Accepted Xth XXXXXXXXX 20XX

DOI: 10.1039/b000000x

A new kind of trinuclear copper(II) motif [Cu_3**L**] was prepared in situ by adopting a multidentate ligand, N'^{2}, $N'^{2'}$-bis(2-hydroxybenzoyl)biphenyl-2,2'-dicarbohydrazide (H_6**L**), in the presence of series N-contained agents. Featuring five different assembly styles, [Cu_3**L**$(DMF)_{2.5}$(hmta)]·$3H_2O$ (**1**), [Cu_3**L**(DMA)(H_2O)(Hmor)] (**2**), [Cu_3**L**$(py)_2$]·DMF (**3**), [Cu_3**L**(DMF)(H_2O)]·2DMF (**4**), [Cu_3**L**(DMA)(H_2O)]·0.5DMA (**5**) (hmta = hexamethylenetetramine, Hmor = morphiline, py = pyridine) were obtained. In these assemblies, the [Cu_3**L**]s are connected with each other into one-dimensional chains via bridging of N-contained agents or via sharing oxygen atom of **L**$^{6-}$ to fuse together. Furthermore, the connecting sytles are found to be governed by the character of the N-contained agents used, which is discussed in detail. Thermal gravimetric analysis and magnetic measurement of some complexes were studied.

Introduction

In the last two decades, coordination supramolecular chemistry has welcome great development because of their potential applications in catalysis,[1] small molecule capture or separation,[2] photoluminescence[3] and imaging,[4] biology,[5] electronics[6] *etc*. In the exploration of novel materials with demanded function, the self-assembly process of coordination supramolecular becomes crucial.[7] Concept of molecular building blocks (MBBs) made complicated self-assembly process become a two-step arrangement.[8] The first step is to build up MBBs with covalent bonds or strong coordination bonds,[9] the second step is to assemble MBBs *via* weak coordination bonds and molecular interactions, such as hydrogen bonds, $\pi\cdots\pi$ stacking, hydrophobic or hydrophilic, van de Walls interactions.[10] Consequently, the design and construction of MBBs is the foundation of supramolecular architecture.

In this paper, we designed a flexible multidentate ligand H_6**L** that embedded with a pair of hydrazides with ten potential coordination atoms. It is well-known that the coordination of hydrazide ligands and metal ions always led to chelated coordination rings, which were stable in solution.[11] Hydrazide-based coordination compounds have shown fascinating properties in magnetism,[12] molecular recognition,[13] biological sensing,[14] etc. As we mentioned above, H_6**L**, which is armed with a pair of hydrazides that spaced by biphenyl group (Scheme 1), might be a good candidate to build up stable coordination motifs, and further assemble into supramolecular networks. Five copper(II) coordination polymers that constructed from **L**$^{6-}$ were harvested by employing different N-contained agents. Based on the analysis and discussion of the synthesis and structure features, the modulation of N-contained agent on the assembly process was presented and discussed.

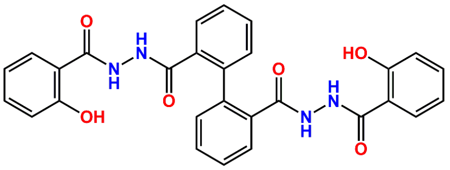

Scheme 1 The structure of H_6**L**.

Experiment section

Reagents and Instruments

Materials used for synthesis were of reagent grade and used without further purification. ^{1}H-NMR (DMSO-d_6) was carried on BRUKER AVANCE III 400 nuclear magnetic resonance spectrometer. IR spectra were recorded in the range of 4000 - 400 cm^{-1} on a Perkin-Elmer FT-IR spectrum 2000 spectrometers using the KBr pellet technique. X-ray powder diffraction (XRPD) measurements were performed on a Rigaku D/max-3c with Cu K_α radiation (λ = 1.5406 Å) in the angular range of 2θ = 5 - 50° at 293K. Elemental analyses were performed by Vario MICRO, CHNOS Elemental Analyzer. The instrument for thermal gravimetric measurements was Netzsch STA 449C Jupiter. Magnetic susceptibility data were collected over the temperature range of 2 - 300 K in magnetic field of 1000 Oe on a MPMS (SQUID)-XL magnetometer. Fluorescence spectrum for H_6**L** was recorded on an Edinburgh Instrument FL/FS-920 fluorescent spectrometer.

Synthesis of the ligand and title complexes

2,2’-biphenyldicarbonyl chloride. Mixture of 2,2-biphenyldicarboxylic acid (1.452 g, 6.0 mmol) and thionyl chloride (10 mL) was refluxed for 9 h, with one drop of DMF (N,N-dimethylformamide). After reaction, solvent and excess thionyl chloride were removed with rotary evaporation, leaving colorless solid of 2,2-biphenyldicarbonyl chloride. Yield: 88.37 %.

N'^{2},N'$^{2'}$-bis(2-hydroxybenzoyl)biphenyl-2,2'-dicarbohydrazide (H_6L). 10 mL DMF solution of 2,2-biphenyldicarbonyl chloride (5.0 mmol) and 10 mL DMF solution of triethylamine (1.4 mL) and salicylhydrazide (13.7 mmol) were mixed with ice-bath. The mixture was warmed to room temperature and refluxed for 9 h. The solvent was removed with reduced pressure distillation to get the crude product as a reddish brown solid. After washed with ethanol for several times, white product was obtained with 78.54 % yield. The product was characterized by ^{1}H-NMR (DMSO-d$_6$), IR spectrum and fluorescence spectrum, which were listed in supplementary information, Fig. S1-S3.

[$Cu_3L(DMF)_{2.5}(hmta)$]·$3H_2O$ (1). H_6**L** (0.0125 mmol, 6.4 mg), $Cu(Ac)_2 \cdot H_2O$ (0.0375 mmol, 7.5 mg) and hmta (hexamethylenetetramine, 0.0375 mmol, 5.3 mg) were mixed and dissolved in 5 mL DMF. Blue rhombic plate-like crystals were obtained in five days, in 13.54 % yield (on the basis of Cu).

[$Cu_3L(DMA)(H_2O)(Hmor)$] (2). H_6**L** (0.0125 mmol, 6.4 mg), $Cu(Ac)_2 \cdot H_2O$ (0.0375 mmol, 7.5 mg) were mixed and dissolved in 5 mL DMA (N,N-dimethylacetamide) with one drop of Hmor (morphiline, ca. 0.58 mmol). Dark blue block shaped crystals were obtained in two months, in 18.31 % yield (on the basis of Cu). IR (KBr, cm^{-1}): 3245w, 3055w, 2973w, 2932w, 2844w, 1600s, 1562m, 1500s, 1464m, 1400s, 1321m, 1250s, 1186m, 1155m, 1109m, 1092m, 1019m, 873m, 852m, 750s, 700m, 637m, 543w, 462m, 433m.

[$Cu_3L(py)_2$]·DMF (3). H_6**L** (0.05 mmol, 25.5 mg) and $Cu(Ac)_2 \cdot H_2O$ (0.15 mmol, 30.4 mg) were mixed and dissolved in 5 mL DMF with one drop of pyridine. Dark blue column-like crystals were obtained in two weeks, in 56.01 % yield (on the basis of Cu). Anal. Calcd. (Found) for $C_{41}H_{33}Cu_3N_7O_7$ (%): C, 52.85 (53.14); H, 3.51 (3.51); N, 10.35; (10.58). IR (KBr, cm^{-1}): 3689w, 3060w, 3005w, 2925w, 2107w, 1675s, 1600s, 1500s, 1450m, 1400s, 1324m, 1253m, 1217m, 1153w, 1091w, 1063m, 901m, 848m, 780m, 754s, 641m, 572w, 437w.

[$Cu_3L(DMF)(H_2O)$]·2DMF (4). H_6**L** (0.025 mmol, 12.8 mg) and $Cu(Ac)_2 \cdot H_2O$ (0.075 mmol, 15.0 mg) were mixed and dissolved in mixed solvent of DMF (3 mL) and acetonitrile (3 mL). Blue columnar crystals were obtained in two weeks, in 37.03 % yield (on the basis of Cu). Anal. Calcd. (Found) for $C_{37}H_{39}Cu_3N_7O_{10}$ (%): C, 47.28 (47.62); H, 4.45 (4.10); N, 8.12; (10.51). IR (KBr, cm^{-1}): 3400w, 3060w, 2928w, 1647s, 1600s, 1564m, 1500s, 1476m, 1406s, 1385s, 1322w, 1230m, 1156m, 1103m, 1048w, 905m, 847m, 756m, 699m, 581w, 545w, 453w.

[$Cu_3L(DMA)(H_2O)$]·0.5DMA (5). The prepration of **5** was similar to that of **4**, but 5 mL DMA that dissolved with piperazine hexahydrate (0.025 mmol, 4.9 mg) was used as solvent instead of the mixed solvent. Blue square plate-like crystals were obtained in two weeks, in 55.74 % yield (on the basis of Cu). Anal. Calcd. (Found) for $C_{68}H_{59}Cu_6N_{11}O_{17}$ (%): C, 48.30 (48.47); H, 4.10 (3.73); N, 9.56; (9.15). IR (KBr, cm^{-1}): 3369w, 3069w, 1603s, 1511s, 1480s, 1397s, 1379s, 1303m, 1227s, 1157m, 1103m, 1046m, 906s, 847s, 750s, 695m, 670m, 595m, 464m, 443m.

Table 1 Crystal data and structure refinement parameters for complex **1–5**

Complex	**1**	**2** ^{a}	**3**	**4**	**5** ^{a}
Formula	$C_{41.5}H_{51.5}Cu_3N_{10.5}O_{11.5}$	$C_{36}H_{36}Cu_3N_6O_9$	$C_{41}H_{33}Cu_3N_7O_7$	$C_{37}H_{39}Cu_3N_7O_{10}$	$C_{68}H_{63}Cu_6N_{11}O_{17}$
Mr	1072.05	887.33	926.36	932.37	1683.50
Crystal system	Monoclinic	Monoclinic	Monoclinic	Monoclinic	Orthorhombic
a/Å	41.720(3)	25.985(5)	14.760(3)	9.6951(19)	22.533(4)
b/Å	8.6534(5)	13.713(3)	14.694(3)	21.832(4)	23.066(5)
c/Å	28.881(2)	24.798(5)	18.395(4)	19.246(4)	14.201(3)
α/°	90	90	90	90	90
β/°	120.329(5)	112.39(3)	98.88(3)	97.76(3)	90
γ/°	90	90	90	90	90
V/Å^3	8999.6(10)	8170(3)	3941.7(14)	4036.4(14)	7381(3)
T/K	113(2)	113(2)	293(2)	293(2)	293(2)
Space group	$C2/c$	$C2/c$	$P2_1/c$	$P2_1/c$	$Pba2$
Z	8	8	4	4	4
R_{int}	0.0602	0.0808	0.0499	0.1194	0.0801
Reflections collected	28465	27620	36450	37325	68086
GOF on F^2	1.050	1.136	0.922	0.959	0.850
R_1 [$I > 2\sigma(I)$] ^{b}	0.0634	0.0746	0.0421	0.0720	0.0535
wR_2 (all data) ^{c}	0.1486	0.1692	0.1233	0.1626	0.1312
Flack Parameter					0.374(14)

[a] The formula and Mr of **2** and **5** in the table are results of excluding the disorded solvent that removed by squeeze process. The overall formula for **2** should be $C_{36}H_{42}Cu_3N_6O_{12}$, with Mr 941.33, F (000) 3868. The overall formula for **5** should be $C_{68}H_{64}Cu_6N_{11}O_{17.5}$, with Mr 1692.50, F (000) 3452.

[b] $R_1 = \Sigma||F_o|-|F_c||/\Sigma|F_o|$.

[c] $wR_2 = [\Sigma w(F_o^2 - F_c^2)^2/\Sigma w(F_o^2)]^{1/2}$.

X-ray Crystallography. Diffraction data for complexes **1** were collected on Agilent technologies SuperNova Micro Focus diffractometer. Diffraction data for complexes **2** and **3** were collected on RIGAKU / SATURN 724 CCD diffractometer. Data for complexes **4 - 5** were collected on Rigaku R-AXIS RAPID diffractometer. All diffractometers were worked by graphite-monochro-matized Mo K_α radiation (λ = 0.71073 Å) using ω scan mode. Absorption coefficients were applied using a multi-scan technique. All the structures were solved by direct method of SHELXS-97 and refined by full-matrix least-squares techniques using SHELX-97 program.[15] Non-hydrogen atoms were refined anisotropically. Hydrogen atoms of organic molecules were generated geometrically and refined by a riding mode. SQUEEZE subroutine of PLATON software suite[16] were applied for the data of complex **2** and **5** to avoid stray diffraction infection. The resulting new HKL files were used to further refinement. A sumary of crystallographic data and structure determination for **1-5** are provided in Table 1.

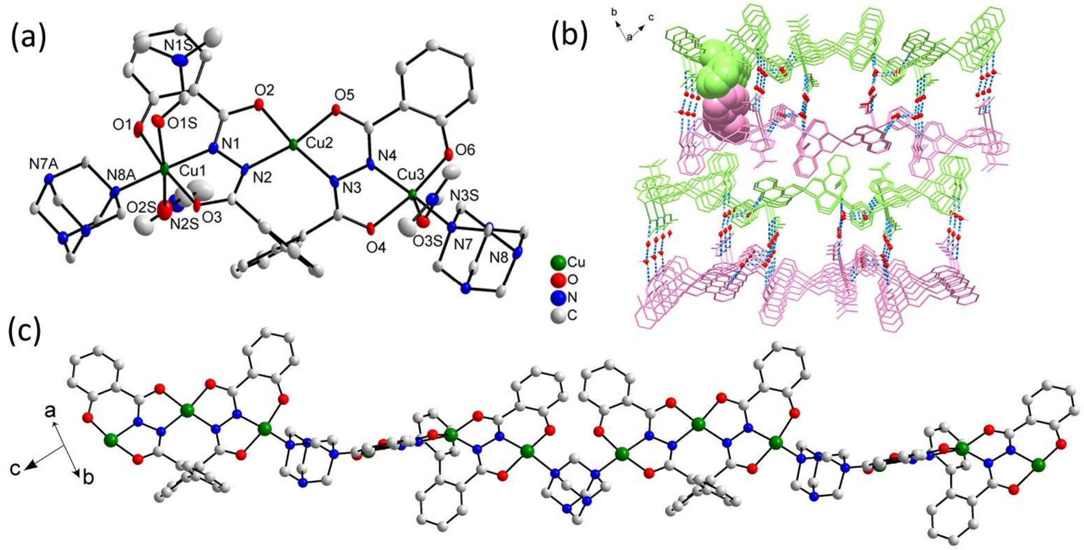

Figure 1 (a) Ellipsoid representation of the coordination environment for Cu^{II} ions in complex **1** (ellipsoid probability 50 %). Hydrogen atoms and lattice solvents are omitted for clarity. Symmetry code: A = x, 2-y, 0.5+z. (b) Side view of the hydrogen bonding bilayers structure for **1** (hydrogen bonds show as blue dashed line). The green or pink chains represent separate one-dimensional structures. The biphenol groups of **L**$^{6-}$ were filled in the void space of bilayers, which was shown in space filling mode in only one channel for clarity. (c) Representation of 1D chain in **1**. Hydrogen atoms and solvents (coordinated and lattice) are omitted for clarity.

Results and discussion

Crystal Structures and Discussion

[Cu$_3$L(DMF)$_{2.5}$(hmta)]·3H$_2$O (1). Complex **1** crystallizes in monoclinic system, space group *C*2/*c*, featuring 1D infinite structure which forms 2D supramolecular bilayer structure by hydrogen bonding. The asymmetric unit for **1** contains three crystallographic unique Cu^{II} ions, one **L**$^{6-}$, one hmta, two and a half DMF molecules, and three lattice water molecules. Three kinds of distinct coordination geometries around Cu^{II} are observed (Figure 1a). Cu1 adopts distorted octahedral geometry. The equatorial plane is completed by three atoms from **L**$^{6-}$ (O1, N1, O3) and one N atom from hmta. Axial positions of the octahedron are occupied by two O atoms from DMF molecules, adopting elongated bond length (2.6367(83) and 2.5011(57) Å), which could attribute to Jahn-Teller effect. Cu2 displays compressed tetrahedral geometry, with two pairs of N and O atoms from **L**$^{6-}$ (O2, O5, N2, O3). The geometry around Cu3 is axially elongated square-pyramid, with three atoms from **L**$^{6-}$ (O4, N4 and O6) and one N atom from hmta, one O atom from DMF.

The as-synthesized ligand is completely deprotonated, behaves as an organic host that embedded with three Cu^{II}, in situ generating [Cu$_3$**L**] motif. As shown in Figure 1c, the [Cu$_3$**L**] motifs are linked by hmta into infinite one-dimensional structure, which means the [Cu$_3$**L**] motifs could serve as MBBs for further assemble if the linker hmta is substitutable. There are multiple hydrogen bonds between lattice water molecules and hmta, DMF, deprotonated hydroxyl groups of **L**$^{6-}$, which direct to supramolecular bilayer structure in (0 1 1) plane. As shown in Figure 1b, the void space in the bilayer structure is filled by the biphenyl group of **L**$^{6-}$.

[Cu$_3$L(DMA)(H$_2$O)(Hmor)] (2). Substitute hmta by Hmor, crystals of **2** were obtained, featuring distinct one-dimensional structure. The asymmetric unit contains three crystallographic unique Cu^{II} ions, one **L**$^{6-}$, one Hmor, one DMA molecule, and one lattice water molecule. Similar [Cu$_3$**L**] motif exists in the structure. Major differences are the coordination geometries around Cu1 and Cu3. Both Cu1 and Cu3 adopt similar distorted square-pyramid geometries. As shown in Figure 2a, the equatorial plane of geometry around Cu1 is completed by three atoms from **L**$^{6-}$ (O1, N1 and O2) and one N atom from Hmor. Axial position is occupied by O atom from DMA molecule. Differently, symmetric relevant Hmor coordinates to Cu3 on the axial site. The equatorial plane of geometry around Cu3 is completed by one water molecule and three atoms from **L**$^{6-}$ (O5, N4 and O6). The resulting one-dimensional structure shows waved chain along *c* axis (Figure 2c). Coordinated water molecules (O1W) serve as hydrogen bonding donor, affording hydrogen bonds with oxygen atoms (O1S) of DMA molecules and deprotonated hydroxyl group (O6) of **L**$^{6-}$, which leads to 2D supramolecular layer structure (Figure 2b).

Compared to the crystal structure of **1**, in which linker hmta connects [Cu$_3$**L**] motifs by a pair of equatorial coordination bonds, the linker Hmor in **2** displays another kind of connecting style by one equatorial bond and one axial bond. To distinguish both assembly styles, we would like to label *Eq-hmta-Eq* for assembly style in **1** and *Eq-Hmor-Ax* for that in **2** respectively.

[Cu$_3$L(py)$_2$]·DMF (3). Complex **3** crystallizes in monoclinic, space group $P2_1/c$. The asymmetric unit contains three crystallographic unique Cu^{II} ions, one **L**$^{6-}$, two pyridine molecules and one lattice DMF molecule. Similar [Cu$_3$**L**] motif is also observed. In [Cu$_3$**L**] motif, both Cu1 and Cu3 display distorted square-pyramidal geometries, with two pyridine molecules coordinate to Cu1 and Cu3 in the equatorial plane respectively (Figure 3a). The axial positions of the geometries around Cu1 and Cu3 are occupied by O atoms from symmetric relevant **L**$^{6-}$. In this way, the [Cu$_3$**L**] motifs are assembled by themselves in a stepwise fashion into one-dimensional structure (Figure 3b). Because the axial coordination bonds play a key role in the assembly, we propose this kind of assembly style as *AxAx*. The 1D chains pack with each other, embedded lattice DMF molecules in void space.

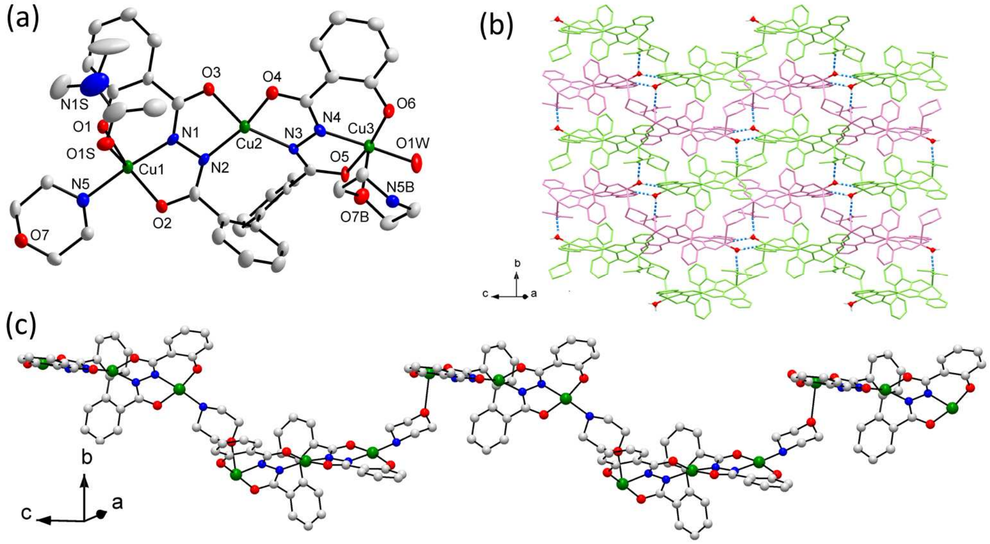

Figure 2 (a) Ellipsoid representation of the coordination environment for Cu^{II} ions in complex **2** (ellipsoid probability 50 %). Hydrogen atoms and lattice solvents are omitted for clarity. Symmetry code: B = x, 2-y, -0.5+z. (b) Top view of the 2D hydrogen bonding structure for **2**. The green or pink waved chains represent separate one-dimensional structures. (c) Representation of 1D chain in **2**. Hydrogen atoms and solvents (coordinated and lattice) are omitted for clarity. Colour scheme is the same as Figure 1.

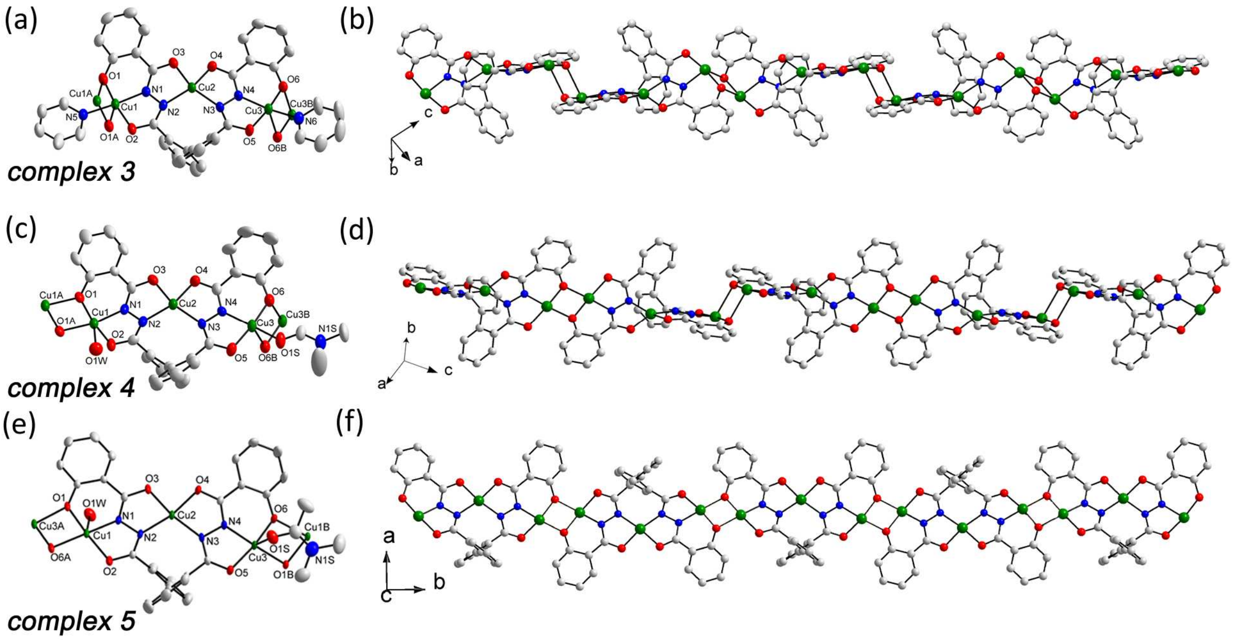

Figure 3 Ellipsoid representations of the coordination environment for Cu^{II} ions (a, c, e) and 1D structures (b, d, f) observed in complex **3**-**5** respectively (ellipsoid probability 50 %). Hydrogen atoms and lattice solvents are omitted for clarity. Colour scheme is the same as Figure 1. Symmetry code: (a) A = 1-x, 1-y, -z, B = 2-x, 1-y, 1-z; (c) A = 1-x, 1-y, 1-z, B = -x, 1-y, 1-z; (e) A = 0.5-x, -0.5+y, z, B = 0.5-x, 0.5+y, z.

[Cu_3L(DMF)(H_2O)]·2DMF (4). The crystal structure for **4** features one-dimensional structures that constructed from the [Cu_3**L**] motif too, however, with different assembly style. The asymmetric unit content includes one [Cu_3**L**] motif, three DMF molecules and one water molecule. As shown in Figure 3c, both Cu1 and Cu3 display distorted square-pyramidal geometries. The axial position of geometry around Cu1 is occupied by water molecule, leaving equatorial position to O1A atom from symmetric relevant $\mathbf{L}^{6-}$. On the other hand, one DMF molecule coordinates to Cu3 equatorially (O1S), leaving the axial position for O6B from another symmetric relevant $\mathbf{L}^{6-}$. Consequently, adjacent [Cu_3**L**] motifs connect with each other via sharing a pair of μ_2-O atoms into one-dimensional structure (Figure 3d). Due to the different coordination environments around Cu1 and Cu3, the assembly style existed in **4** could be labelled as *EqAx*.

[Cu_3L(DMA)(H_2O)]·0.5DMA (5). X-ray single crystal diffraction analysis reveals that **5** crystallized in non-centrosymmetric space group *Pba*2. The asymmetric unit content includes two [Cu_3**L**] motifs, three DMA molecules and two water molecules. The two [Cu_3**L**] motifs feature similar structures and assembly styles, so only one of them will be described herein. As shown in Figure 3e, both Cu1 and Cu3 display distorted square-pyramidal geometries, with one water molecule and one DMA molecule coordinated to Cu1 and Cu3 respectively on the axial position. There are μ_2-O atoms (O6A and O1B) that coordinated to Cu1 and Cu3 in the equatorial plane, leading [Cu_3**L**] motifs to fuse with each other (Figure 3f). The assembly style found in complex **5** should be labelled as *EqEq* style.

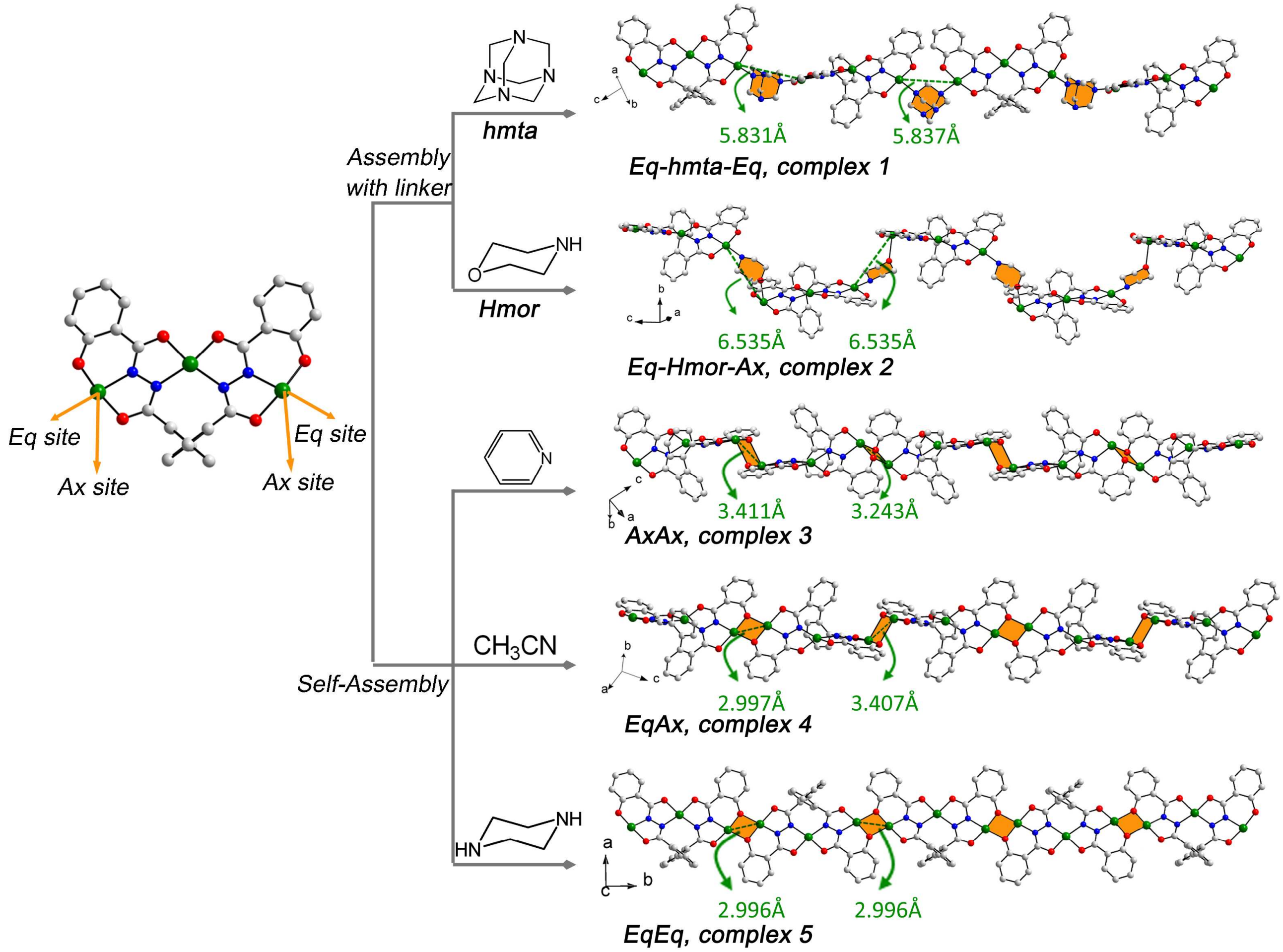

Figure 4 The assembly of [Cu_3**L**] motif modulated by N-contained agents. On the left, the diagram represents a typical structure of [Cu_3**L**] motif with orange arrows indicating the active coordination sites. "*Eq* site" means potential equatorial assembly style, while "*Ax* site" means potential axial assembly style. On the right, the differences among complex **1-5** were highlighted with orange colour areas which represent linkers (complex **1** and **2**) or joints (complex **3-5**). Green dash line and numbers in green represent the Cu···Cu distances. Colour scheme for atoms is the same as Figure 1.

Synthesis and Structural Discussion. The bihydrazide ligand H_6**L** is a multidentate compound which offers up to ten available coordination atoms. Structural analysis of complex **1-5** revealed that deprotonated $\mathbf{L}^{6-}$ could form ten coordination bonds with three Cu^{II}, leading to [Cu_3**L**] motif. As shown in Figure 4, the [Cu_3**L**] motif in **1-5** shows four active coordination sites for further assembly. Considering the typical elongated Jahn-Teller effect of Cu^{II} coordination geometry, the equatorial coordination bond length of Cu^{II} would be shorter than axial one (tables of bond length for **1-5** were listed in supplementary information), the strength of equatorial bond must be stronger than axial bond. Consequently, the involved N-contained agent, which is coordination available, is possible to play a key role in the assembly of [Cu_3**L**] motif. In our study, hmta, Hmor, pyridine, acetonitrile, and piperazine, with diverse coordination abilities and structural features were introduced, directing to five kinds of assembly styles. It should be mentioned that although DMF and DMA are also N-contained agents, but this paper won't discuss their influence, because their property are similar, and they are major solvent in the synthesis of each complex.

First, the N-contained agents play as linkers in the assembly of [Cu_3**L**] motifs, exhibiting *Eq-hmta-Eq* (complex **1**) and *Eq-Hmor-Ax* (complex **2**) styles. Hmta features adamantine-like structure, offering identical four tertiary amines for coordination. Those tertiary amines are competitive to coordinate with Cu^{II} in equatorial sites. However, it is hard for hmta behaves as three-connected or four-connected linker because of the steric effect of [Cu_3**L**] motif. In practical, two tertiary amines are observed to coordinate with [Cu_3**L**] motif equatorially, resulting *Eq-hmta-Eq* style for **1**. While Hmor features boat-shaped conformation, offering a secondary amine and an ether group, which is less competitive ligand. Maybe because the Hmor was added greatly excess, both amine and ether groups of Hmor coordinate with Cu^{II}. Ether group, which has lower reaction activity, coordinates with Cu^{II} on the axial site, while the secondary amine coordinates equatorially. As a result, the assembly style for [Cu_3**L**] motif that existed in **2** is *Eq-Hmor-Ax*.

Second, the N-contained agents play as structure directing agents, leading to the self-assembly of [Cu_3**L**] motifs. The [Cu_3**L**] motifs were assembled by themselves through a pair of μ_2-O bridging, showing *AxAx*, *EqAx*, *EqEq* styles in the structures of **3-5**. The choice of these styles is also related to the coordination ablity of the N-contained agents. In the structure of complex **3**, pyridine, which is a good candidate to coordinate with Cu^{II}, occupys both equatorial active sites of [Cu_3**L**] motif. As a result, the assembly of [Cu_3**L**] motifs in **3** is *AxAx* style. When the N-contained agent is acetonitrile or piperazine, complex **4** or **5** is harvested respectively, although their crystal structures don't contain these agents. Further experiments showed that if without acetonitrile or piperazine in the reaction, complex **4** or **5** would not be harvested, which indicates both agents might be structure directing agents. The coordination abilities of acetonitrile and piperazine are weaker than pyridine. However, the large amount of acetonitrile may make a good chance for acetonitrile coordinate to Cu^{II} randomly, which give rise to the existence of *EqAx* assembly style for **4**. It is worth to mention that, crystals of complex **4** were not easy to reproduce, which might indicate the *EqAx* style be an "unstable state" in the assembly process. The *EqEq* assembly style exists in **5**, which might attribute to the weak coordination ability and small amount of addition of piperazine.

As shown in Figure 4, the diverse assembly styles of [Cu_3**L**] motifs give rise to various Cu···Cu distances between two adjacent [Cu_3**L**] motifs. It is obviously that self-assembly of [Cu_3**L**] motifs brings in closer Cu···Cu distance. The minimum value of Cu···Cu distance is 2.996 Å with *EqEq* assembly style for complex **5**.

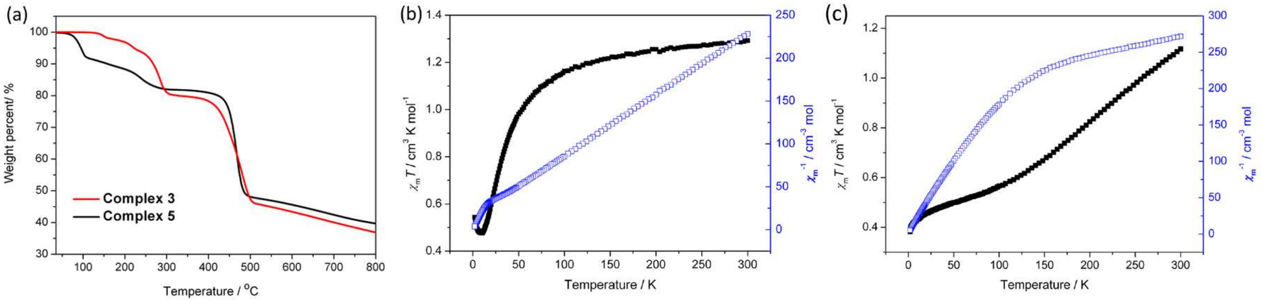

Figure 5 (a) The thermal gravimetric curves for complex **3** (red line) and **5** (black line). (b, c) Temperature dependence curves of $\chi_m T$ (■) and χ_m^{-1} (□) for complex **3** (b) and **5** (c).

Thermal Stabilities and Magnetism Study

Owing to the low yield of complex **1** and **2**, only complex **3-5** were studied by X-ray powder diffraction (XRPD) to confirm the pure phase (Fig. S4-S6 in ESI). Further investigation on thermal stabilities and magnetism were carried out for complex **3** and **5**, the two complexes with distinct assembly styles (*AxAx* for **3**, *EqEq* for **5**).

Upon heating from room temperature, complex **3** stays stable upon heating up to 120 °C. When temperature goes higher, obvious weight loss (19.7%) exists in the range of 120 °C to 310 °C, which is lower than theoretical value (25.0%) for the sum of DMF (7.9%) and pyridine molecules (17.1%). That might attribute to the stable coordination bonds of Cu^{II} and nitrogen atoms from pyridine (bond distances 2.014(3) and 2.006(3) Å in Table S7). There is slight weight loss in the range of 310 °C (80.3%) to 380 °C (79.1%), followed by a sharp decline when temperature gets higher, which means the decomposition temperature for **3** is about 380 °C. Similar thermal stability study was taken for complex **5** as well. Upon heating from room temperature, complex **5** sample loses weight gradually, with 17.6% mass loss before 280 °C (Figure 5a), corresponding to the contained solvent molecules (theoretical value 17.7%). In the range of 280 °C to 400 °C, there is a platform. When temperature is higher than 400 °C, significant weight loss exists, indicating complex **5** might decompose at 400 °C. Comparing two thermal gravimetric curves, **5** shows better thermal stability than **3**, which indicates that the *EqEq* assembly style for **5** benefits the thermal stability.

Magnetic behaviors of complex **3** and **5** are depicted in Figure 5 in the form of $\chi_m T$ vs. T and χ_m^{-1} vs. T. For complex **3**, the room temperature value for $\chi_m T$ is 1.29 $cm^3 \cdot mol^{-1} \cdot K$, which is slightly higher than that of three non-interacting Cu^{II} with S = 1/2 (1.125 $cm^3 \cdot mol^{-1} \cdot K$). Upon cooling, the value of $\chi_m T$ decreases gradually. When the temperature is lower than 100 K, $\chi_m T$ value decreases significantly, reaching a minimum value of 0.48 $cm^3·mol^{-1}·K$ at 10 K. There is an increase from 10 K to 2 K, with χ_mT value from 0.48 to 0.54 $cm^3·mol^{-1}·K$. Curve of χ_m^{-1} vs. T for complex **3** follows Curie–Weiss law above 46 K, with C = 1.40 $cm^3·mol^{-1}·K$ and θ = –20.5 K, which indicates the antiferromagnetic property of complex **3**.

The magnetic behavior upon cooling for complex **5** is significantly different from complex **3**. Value of χ_mT at 300 K is 1.12 $cm^3·mol^{-1}·K$, which is close to the theoretical value of three non-interacting Cu^{II} with S = 1/2 (1.125 $cm^3·mol^{-1}·K$). The decline slope for $\chi_mT \sim T$ curve of complex **5** in the range of 300 K to 100 K is larger than that for complex **3**. A minimum χ_mT value (0.38 $cm^3·mol^{-1}·K$) exists at 2 K. Curve of χ_m^{-1} vs. T follows Curie–Weiss law above 152 K, with Curie constant C = 3.38 $cm^3·mol^{-1}·K$ and Weiss constant θ = –623.7 K, which indicates strong antiferromagnetic property.

Both complexes feature negative Weiss constant, while the absolute value are greatly different, which could be attributed to the different assembly styles in crystal structures. As we discussed above, the *EqEq* style in **5** exists minimum value of Cu···Cu distance 2.996 Å, while that values for *AxAx* style in **3** are 3.411 and 3.243 Å. This difference might explain the reason for larger absolute value of Weiss constant for **5** than that for **3**.

Conclusions

Five coordination polymers that based on a multidentate bihydrazide ligand H_6**L** and Cu^{II} were synthesized and characterized, which bring in the study of the assembly of a new kind of [Cu_3**L**] motif. The [Cu_3**L**] motif shows four active coordination sites, directing the assembly styles be modulated by the coordination ability of involved N-contained agents. Complex **3** and **5** showed good thermal stabilities and antiferromagnetic property, especially **5**. Upon above study, [Cu_3**L**] motif has shown promising ability in the modulated assembly of coordination supramolecular chemistry.

Acknowledgments

We thank the financial support from the National Natural Science Foundation of China (21001026 and 61008040), the State Key Laboratory of Structural Chemistry, Fujian Institute of Research on the Structure of Matter, Chinese Academy of Sciences (20110006 and 20140010) and the Startup Fund (022220) of Fuzhou University.We thank Prof. Long's lab in Xiamen University for technical support.

Notes and references

[a] *College of Chemistry, Fuzhou University, Fuzhou, 350116, PR China. E-mail: shutingwu@fzu.edu.cn*

[b] *State Key Laboratory of Structural Chemistry, Fujian Institute of Research on the Structure of Matter, Chinese Academy of Sciences, Fuzhou, Fujian 350002, PR China.*

† Characterziation of H_6**L,** XRPD patterns and bond length lists of complex **1-5** are available in Electronic Supplementary Information (ESI). CCDC numbers 983125-983126, and 983128-983130. For ESI and crystallographic data in CIF or other electronic format see DOI: 10.1039/b000000x/

1 (a) M. Raynal; P. Ballester, A. Vidal-Ferran, P. W. N. M. van Leeuwen, *Chem. Soc. Rev.*, 2014, **43**, 1660-1733. (b) P. Dydio, R. J. Detz, J. N. H. Reek, *J. Am. Chem. Soc.*, 2013, **135**, 10817-10828. (c) N. C. Gianneschi, M. S. III Masar, C. A. Mirkin, *Acc. Chem. Res.*, 2005, **38**, 825-837. (d) M. Yoshizawa, Y. Takeyama, T. Kusukawa, M. Fujita, *Angew. Chem., Int. Ed.*, 2002, **41**, 1347-1349.

2 (a) Z. Zhang, L. Wojtas, M. Eddaoudi, M. J. Zaworotko, *J. Am. Chem. Soc.*, 2013, **135**, 5982-5985. (b) P. D. Frischmann, M. J. MacLachlan, *Chem. Soc. Rev.*, 2013, **42**, 871-890. (c) C. C. Huang, J. J. Liu, Y. Chen, M. J. Lin, *Chem. Commun.*, 2013, **49**, 11512-11514. (d) R. Galassi, S. Ricci, A. Burini, A. Macchioni, L. Rocchigiani, F. Marmottini, S. M. Tekarli, V. N. Nesterov, M. A. Omary, *Inorg. Chem.*, 2013, **52**, 14124-14137. (e) I. Bassanetti, F. Mezzadri, A. Comotti, P. Sozzani, M. Gennari, G. Calestani, L. Marchio, *J. Am. Chem. Soc.*, 2012, **134**, 9142-9145.

3 (a) J. Yu, Y. Cui, H. Xu, Y. Yang, Z. Wang, B. Chen, G. Qian, *Nat. Commun.*, 2013, **4**, 2719/1-2719/7. (b) J. He, M. Zeller, A. D. Hunter, Z. Xu, *J. Am. Chem. Soc.*, 2012, **134**, 1553-1559. (c) J. Jankolovits, C. M. Andolina, J. W. Kampf, K. N. Raymond, V. L. Pecoraro, *Angew. Chem., Int. Ed.*, 2011, **50**, 9660-9664. (d) G. Clavier, P. Audebert, *Chem. Rev.*, 2010, **110**, 3299-3314.

4 (a) D. Liu, K. Lu, C. Poon, W. Lin, *Inorg. Chem.*, 2014, **53**, 1916-1924. (b) J. H. Xu, F. P. Gao, X. F. Liu, Q. Zeng, S. S. Guo, Z. Y. Tang, X. Z. Zhao, H. Wang, *Chem. Commun.*, 2013, **49**, 4462-4464. (c) J. D. Rocca, D. Liu, W. Lin, *Acc. Chem. Res.*, 2011, **44**, 957-968. (d) P. Horcajada, T. Chalati, C. Serre, B. Gillet, C. Sebrie, T. Baati, J. F. Eubank, D. Heurtaux, P. Clayette, C. Kreuz, J.-S. Chang, Y. K. Hwang, V. Marsaud, P.-N. Bories, L. Cynober, S. Gil, G. Férey, P. Couvreur, R. Gref, *Nature Mater.*, 2010, **9**, 172–178.

5 (a) T. R. Cook, V. Vajpayee, M. H. Lee, P. J. Stang, K.-W. Chi, *Acc. Chem. Res.*, 2013, **46**, 2464-2474. (b) B. Kowalewski, J. Poppe, U. Demmer, E. Warkentin, T. Dierks, U. Ermler, K. Schneider, *J. Am. Chem. Soc.*, 2012, **134**, 9768-9774. (c) D. T. Quang, J. S. Kim, *Chem. Rev.*, 2010, **110**, 6280-6301.

6 (a) A. A. Talin, A. Centrone, A. C. Ford, M. E. Foster, V. Stavila, P. Haney, R. A. Kinney, V. Szalai, G. El, Y. Farid, P. Heayoung, et al. *Science*, 2014, **343**, 66-69. (b) G. Givaja, P. Amo-Ochoa, C. J. Gomez-Garcia, F. Zamora, *Chem. Soc. Rev.*, 2013, **41**, 115-147.

7 (a) M. Malakoutikhah, J. J.-P. Peyralans, M. Colomb-Delsuc, H. Fanlo-Virgos, M. C. A. Stuart, S. Otto, *J. Am. Chem. Soc.*, 2013, **135**, 18406-18417. (b) X. Lu, X. Li, Y. Cao, A. Schultz, J.-L. Wang, C. N. Moorefield, C. Wesdemiotis, S. Z. D. Cheng, G. R. Newkome, *Angew. Chem. Int. Ed.*, 2013, **52**, 7728-7731. (c) A. B. Lago, R. Carballo, S. Rodríquez-Hermida, E. M. Vázquez-López, *CrystEngComm*, 2013, **15**, 1563-1570.

8 (a) T. R. Cook, Y.-R. Zheng, P. J. Stang, *Chem. Rev.*, 2013, **113**, 734-777. (b) H.-Y. Gong, B. M. Rambo, V. M. Lynch, K. M. Keller, J. L. Sessler, *J. Am. Chem. Soc.*, 2013, **135**, 6330-6337. (c) S. K. Elsaidi, M. H. Mohamed, L. Wojtas, A. J. Cairns, M. Eddaoudi, M. J. Zaworotko, *Chem. Commun.*, 2013, **49**, 8154-8156. (d) G. J. McManus, Z. Q. Wang, D. A. Beauchamp, M. J. Zaworotko, *Chem. Commun.*, 2007, 5212-5213. (e) L. Öhrström, K. Larsson, *Dalton Trans.*, 2004, 347-353.

9 (a) M. Paul, N. N. Adarsh, P. Dastidar, *Cryts. Growth Des.*, 2014, **14**, 1331-1337. (b) K. T. Mahmudov, M. N. Kopylovich, A. J. L. Pombeiro, *Coord. Chem. Rev.*, 2013, **257**, 1244-1281. (c) M. D. Wise, A. Ruggi, M. Pascu, R. Scopelliti, K. Severin, *Chem. Sci.*, 2013, **4**, 1658-1662. (d) M. Frank, J. Hey, I. Balcioglu, Y.-S. Chen, D. Stalke, T. Suenobu, S. Fukuzumi, H. Frauendorf, G. H. Clever *Angew. Chem. Int. Ed.*, 2013, **52**, 10102-10106.

10 (a) S. S. Mondal, A. Bhunia, A. Kelling, U. Schilde, C. Janiak, H.-J. Holdt, *J. Am. Chem. Soc.*, 2014, **136**, 44-47. (b) H. T. Chifotides, K. R. Dunbar, *Acc. Chem. Res.*, 2013, **46**, 894-906. (c) D. J. Wolstenholme, J. Flogeras, F. N. Che, A. Decken, G. S. McGrady, *J. Am. Chem. Soc.*, 2013, **135**, 2439-2442. (d) S. Lipstman, I. Goldberg, *Cryst. Growth Des.*, 2013, **13**, 942-952. (e) D. Salazar-Mendoza, J. Cruz-Huerta, H. Hopfl, I. F. Hernandez-Ahuactzi, M. Sanchez, *Cryst. Growth Des.*, 2013, **13**, 2441-2454.

11 (a) F. Hengesbach, X. Jin, A. Hepp, B. Wibbeling, E.-U. Wuerthwein, W. Uhl, *Chem. Eur. J.*, 2013, **19**, 13901-13909. (b) A. Trzesowska-Kruszynska, *Cryst. Growth Des.*, 2013, **13**, 3892-3900. (c) Z.-Z. Wen, X.-L. Wen, S.-L. Cai, S.-R. Zheng, J. Fan, W.-G. Zhang, *CrystEngComm.*, 2013, **15**, 5359-5367. (d) P.

Krishnamoorthy, P. Sathyadevi, R. R. Butorac, A. H. Cowley, N. S. P. Bhuvanesh, N. Dharmaraj, *Dalton Trans.*, 2012, **41**, 6842-6854. (e) A. Jamadar, A. K. Duhme-Klair, K. Vemuri, M. Sritharan, P. Dandawatec, S. Padhye, *Dalton Trans.*, 2012, **41**, 9192-9201. (f) M. J. Prakash, M. S. Lah, *Chem. Commun.*, 2009, 3326–3341. (g) D. Moon, J. Song, M. S. Lah, *CrystEngComm.*, 2009, **11**, 770-776. (h) X. F. Liu, W. L. Liu, K. Lee, M. Park, H. C. Ri, G. H. Kimd, M. S. Lah, *Dalton Trans.*, 2008, 6579-6583. (i) D. Moon, K. Lee, R. P. John, G. H. Kim, B. J. Suh, M. S. Lah, *Inorg. Chem.*, 2006, **45**, 7991-7993. (j) S.-X. Liu, S. Lin, B.-Z. Lin, C.-C. Lin, J.-Q. Huang, *Angew. Chem. Int. Ed.*, 2001, **40**, 1084-1087. (k) J. Choi, J. Park, M. Park, D. Moon, M. S. Lah, *Eur. J. Inorg. Chem.*, 2008, **35,** 5465-5470.

12 (a) V. Chandrasekhar, S. Hossain, S. Das, S. Biswas, J.-P. Sutter, *Inorg. Chem.*, 2013, **52**, 6346-6353. (b) L. Zou, L. Zhao, P. Chen, Y.-N. Guo, Y. Guo, Y.-H. Li, J. Tang, *Dalton Trans.*, 2012, **41**, 2966-2971. (c) M. S. Shongwe, S. H. Al-Rahbi, M. A. Al-Azani, A. A. Al-Muharbi, F. Al-Mjeni, D. Matoga, A. Gismelseed, I. A. Al-Omari, A. Yousif, H. Adams, M. J. Morris, M. Mikuriya, *Dalton Trans.*, 2012, **41**, 2500-2514.

13 (a) Y. Liu, X. Lv, Y. Zhao, J. Liu, Y.-Q. Sun, P. Wang, W. Guo, *J. Mater. Chem.*, 2012, **22**, 1747-1750. (b) W. Huang, C. Song, C. He, G. Lv, X. Hu, X. Zhu, C. Duan, *Inorg. Chem.*, 2009, **48**, 5061-5072.

14 (a) P. Krishnamoorthy, P. Sathyadevi, R. R. Butorac, A. H. Cowley, N. S. P. Bhuvanesh, N. Dharmaraj, *Dalton Trans.*, 2012, **41**, 4423-4436. (b) P. J. Deuss, G. Popa, C. H. Botting, W. Laan, P. C. J. Kamer, *Angew. Chem. Int. Ed.*, 2010, **49**, 5315-5317.

15 G. M. Sheldrick, *Acta Cryst.*, 2008, **A64**, 112-122.

16 A. L. Spek, *PLATON, A Multipurpose Crystallographic Tool, Utrecht University, Utrecht, The Netherlands.* 2008.

Graphical Abstract for

Delicate modulated assembly of a new kind of trinuclear copper(II) motifs governed by N-contained agents

Shu-Ting Wu,*[a,b] Hong-Liang Tang,[a] Shu-Mei Lu,[a] Qiao-Yan Ye,[a] Xi-He Huang,[a,b] Chang-Cang Huang,[a] Xiao-Lin Hu,[a] Shou-Tian Zheng[a]

a: College of Chemistry, Fuzhou University, Fuzhou, 350116, PR China
b: State Key Laboratory of Structural Chemistry, Fujian Institute of Research on the Structure of Matter, Chinese Academy of Sciences, Fuzhou, Fujian 350002, PR China

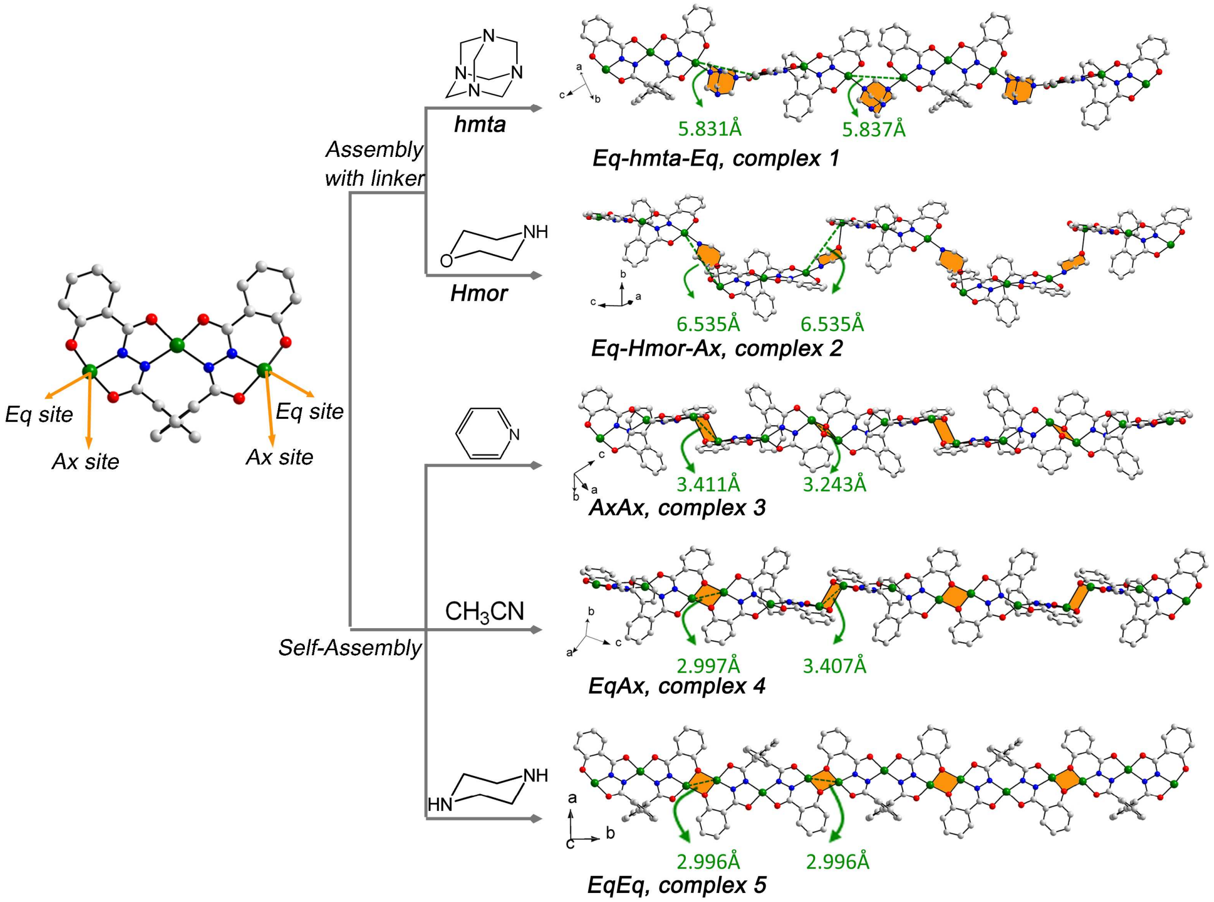

A new kind of trinuclear cupric motif was prepared in situ by adopting a novel multidentate bihydrazide ligand, leading to five assembly styles that governed by N-contained agents.